

# The Interaction of $\text{CF}_3\text{CH}_2\text{OH}$ and $(\text{CF}_3\text{CF}_2)_2\text{O}$ with Amorphous Carbon Films

Nisha Shukla<sup>†</sup> and Andrew J. Gellman\*

Department of Chemical Engineering, Carnegie Mellon University,  
Pittsburgh, Pennsylvania 15213

Jing Gui

Seagate Technology, Inc., Fremont, California 94538

Received March 23, 2000. In Final Form: May 15, 2000

Fluorinated alcohols and fluorinated ethers adsorbed on carbon films have been studied in order to model the surface chemistry of Fomblin Zdol lubricants on the carbon-coated surfaces of magnetic data storage media. The model compounds used were 2,2,2-trifluoroethanol ( $\text{CF}_3\text{CH}_2\text{OH}$ ), which is representative of the end groups of Fomblin Zdol, and perfluorodiethylether  $(\text{CF}_3\text{CF}_2)_2\text{O}$ , which represents the main chain of Fomblin Zdol. Temperature-programmed desorption (TPD) spectroscopy was used to measure the desorption energies of these compounds on a variety of different carbon films. Desorption energies were measured on amorphous hydrogenated carbon (a- $\text{CH}_x$ ), amorphous nitrogenated carbon (a- $\text{CN}_x$ ), cathodic arc carbon (CAC), and ion-beam sputtered carbon (IBC). On all carbon film surfaces the desorption energy of  $\text{CF}_3\text{CH}_2\text{OH}$  is higher than that of  $(\text{CF}_3\text{CF}_2)_2\text{O}$ . The desorption energy of  $\text{CF}_3\text{CH}_2\text{OH}$  is higher on the a- $\text{CN}_x$  films than on the other carbon films; however, the desorption energy of  $(\text{CF}_3\text{CF}_2)_2\text{O}$  does not depend on the type of carbon. Finally, the desorption energies are dependent upon  $\text{CF}_3\text{CH}_2\text{OH}$  and  $(\text{CF}_3\text{CF}_2)_2\text{O}$  coverage, indicating that the carbon films are heterogeneous and expose binding sites with a range of affinities for adsorption. Systematic measurements of the desorption energies over a range of coverages have been used to map out the heterogeneity of all the carbon films.

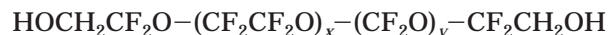
## Introduction

In recent years research in the disk drive industry has been directed primarily toward achieving higher areal densities of stored data. In part this is achieved by decreasing the flying height between the read–write head and the hard disk surface. In addition, there is also a demand for faster access to data and faster data transfer, both of which require higher disk spin rates. This requires improved tribological performance of the head–disk interface.<sup>1</sup> The magnetic storage layer on the disk surface is protected from contact with the read–write head by a thin amorphous carbon film coated with an ultrathin film of perfluoropolyalkylether (PFPE) lubricant. Since, in the future, there will be room for only a single molecular monolayer of the lubricant on the disk surface, its interactions with the carbon film will dictate its properties as a lubricant. In this work we have focused on understanding the molecular level interaction of PFPE lubricants with carbon films.

A number of different types of carbon films have been used or considered for use to protect the surfaces of data storage media. These include amorphous hydrogenated carbon (a- $\text{CH}_x$ ), amorphous nitrogenated carbon (a- $\text{CN}_x$ ), cathodic arc carbon (CAC), and ion-beam sputtered carbon (IBC).<sup>2,3</sup> These are sputtered or deposited by other methods onto the surface of the magnetic layer as thin films (<100 Å). The purpose of the carbon film is to provide wear protection for the magnetic layer if it comes into contact with the read–write head and to provide corrosion protection for the magnetic layer. Since the chemical

compositions and characteristics of these carbon films differ, it is important to understand the effects that these differences may have on their interactions with the PFPE lubricant films.

PFPEs are commonly used as disk surface lubricants because of their unique physical and chemical properties. PFPEs are highly inert at temperatures up to 650 K. Low-temperature (370 K) decomposition requires the presence of Lewis acids such as  $\text{AlCl}_3$  and  $\text{SbF}_5$ .<sup>4,5</sup> In addition, these polymers have low viscosity and low volatility, which makes them suitable as lubricants in the magnetic recording and aerospace industries. In data storage applications the carbon film which has been sputtered onto the magnetic layer of the disk is coated with the PFPE. This combination of lubricant and carbon overcoat provides adequate wear protection for the magnetic layer and prevents the read–write head from “crashing” on the hard disk surface. The most commonly used PFPE is Fomblin Zdol, which has a perfluorinated ether backbone terminated at either end by hydroxyl groups.



The interactions of the ether linkages and the hydroxyl end groups of Fomblin Zdol with the carbon films influence its properties as a lubricant.

Several studies have addressed the nature of the bonding of fluoroethers to carbon films.<sup>6–9</sup> The fluoro

(4) Sianesi, D.; Zamboni, V.; Fontanelli, R.; Binagli, M. *Wear* **1971**, 18, 85.

(5) Kasai, P. H.; Tang, W. T.; Wheeler, P. *Appl. Surf. Sci.* **1991**, 51, 201.

(6) Merchant, K.; Mee, P.; Smallen, M.; Smith, S. *IEEE Trans. Magn.* **1990**, 26, 2688.

(7) Gao C.; Dai, P. *IEEE Trans Magn.* **1997**, 33, 3118.

(8) Cornaglia, L.; Gellman, A. J. *J. Vac. Sci. Technol.* **1997**, A 15, 2755.

\* To whom correspondence should be addressed.

<sup>†</sup> Current address: Seagate Research Center, Pittsburgh, PA.

(1) Mate, C. M. *Trib. Lett.* **1998**, 4(2), 119.

(2) Hsia-chu, T.; Bogy, D. B. *J. Vac. Sci. Technol.* **1987**, A 5(6), 3287.

(3) Dai, P.; Gao, C. *IEEE Trans. Magn.* **1998**, 34, 1738.

ethers serve as models for the backbone ether linkages of Fomblin Zdol. Comparison of the desorption energies of hydrocarbon and fluorocarbon ethers on a set of a-CH<sub>x</sub> films revealed that the desorption energies of the fluorocarbon ethers are always lower than those of their hydrocarbon analogues. The implication of this is that the bonding of the ethers to the carbon films occurs through the donation of electrons from the lone pairs on the oxygen atom to some unknown groups on the surface of the amorphous carbon film.

The adsorption of alcohols on carbon films has been used to study the bonding of the hydroxyl end groups of Fomblin Zdol to the carbon films. This occurs through a different mechanism than the bonding of ethers.<sup>10</sup> Previous work comparing the desorption energies of hydrocarbon and fluorocarbon alcohols on a-CN<sub>x</sub> and a-CH<sub>x</sub> films has shown that the desorption energies of the fluorocarbon alcohols are always higher than those of the hydrocarbon alcohols. This is opposite to the effect of fluorination on the desorption energies of the ethers. The implication of the observation that fluorination increases the desorption energy of the alcohols is that the mechanism of interaction with the carbon films is one of hydrogen bonding.

The carbon films used in data storage applications have a variety of compositions. Most are sputtered in environments containing either hydrogen or nitrogen and thus have various concentrations of hydrogen or nitrogen incorporated into their structures. The composition of the film surface must influence the chemical interactions of the PFPE lubricant with the film. In thinking about the interactions of the PFPEs with the surfaces of the carbon films it is important to remember that before the PFPE is coated onto the disk, the carbon film is exposed to ambient air and as a result is partially oxidized. The intent of this paper has been to explore the effects of carbon film composition and deposition method on their interactions with PFPEs.

One of the controllable characteristics of the carbon films is the concentration of hydrogen in the film. A previous study of the effects of a-CH<sub>x</sub> composition on the interactions with the PFPE attempted to systematically reduce the hydrogen content of the films by annealing at increasing temperatures (550, 600, 650, and 700 K).<sup>8</sup> The loss of hydrogen during annealing was observed using mass spectrometry. The heating caused a systematic increase in the strength of the interaction of fluorinated ethers with the a-CH<sub>x</sub>. One of the questions that was raised by that study was whether heating of the film only caused hydrogen removal or also caused other changes. The work described in this paper has measured the desorption energies of CF<sub>3</sub>CH<sub>2</sub>OH and (CF<sub>3</sub>CF<sub>2</sub>)<sub>2</sub>O on a set of carbon films that have been prepared with different hydrogen concentrations. These measurements show that the previously observed effects of heating on the fluoroether desorption energies are not solely due to the reduction of hydrogen content.

Previous studies of the adsorption of ethers and alcohols on the surfaces of amorphous carbon films have shown that the surfaces are heterogeneous.<sup>8,10</sup> Desorption experiments using various different initial coverages of the ethers and alcohols have shown that the desorption energy decreases with increasing coverage. This effect could be due to repulsive interactions between adsorbed molecules. However, the interactions between adsorbed ethers on

Cu(111) surfaces and on graphite surfaces, both of which are very homogeneous, have been shown to be slightly attractive rather than repulsive.<sup>11,12</sup> It seems likely, therefore, that the coverage dependent desorption energy of ethers on the a-CH<sub>x</sub> surfaces is due to heterogeneity and the presence of a variety of different ether adsorption sites. The presence of different types of binding sites is not surprising given that the a-CH<sub>x</sub> films are not single crystalline and are known to be partially oxidized. One of the goals of the work described in this paper has been to use desorption measurements to map out the binding site or binding affinity distributions for both fluorinated ethers and alcohols on carbon films of various types and compositions.

This paper describes the results of a series of experiments which have measured the desorption energies of (CF<sub>3</sub>CF<sub>2</sub>)<sub>2</sub>O and CF<sub>3</sub>CH<sub>2</sub>OH adsorbed at various coverages on a set of sputtered carbon films. One major result is that the desorption energies of (CF<sub>3</sub>CF<sub>2</sub>)<sub>2</sub>O do not depend significantly of the composition of the carbon films. In contrast, the desorption energies of CF<sub>3</sub>CH<sub>2</sub>OH are similar on the a-CH<sub>x</sub>, CAC, and IBC films but slightly higher on the a-CN<sub>x</sub> films. In all cases the desorption energy of CF<sub>3</sub>CH<sub>2</sub>OH is greater than that of (CF<sub>3</sub>CF<sub>2</sub>)<sub>2</sub>O. Finally, although all the films are heterogeneous, the distributions of binding site energies are quite similar. These results have been used to give further insight into the bonding of the PFPE lubricants such as Fomblin Zdol to amorphous carbon films.

## 2. Experimental Section

The experiments were carried out in a stainless steel ultrahigh vacuum chamber with a base pressure of  $4 \times 10^{-11}$  Torr which was achieved by using a cryopump and a titanium sublimation pump. The chamber was equipped with two leak valves with  $3/8$  in. diameter stainless steel dosing tubes for introducing the (CF<sub>3</sub>CF<sub>2</sub>)<sub>2</sub>O and CF<sub>3</sub>CH<sub>2</sub>OH vapor into the chamber for adsorption onto the surfaces of the carbon films. The thermally programmed desorption (TPD) experiment used an Ametek Dycor MA200M quadrupole mass spectrometer which allowed five *m/q* ratios to be recorded simultaneously.

The samples used in this work were provided by Seagate Technology, Inc. and the Department of Mechanical Engineering at the University of California at Berkeley. The samples consisted of 3.5 in. aluminum hard disks sputter-coated using various methods with different types of carbon films. Four types of carbon films were used: amorphous hydrogenated carbon (a-CH<sub>x</sub>), amorphous nitrogenated carbon (a-CN<sub>x</sub>), cathodic arc carbon (CAC), and ion beam sputtered carbon (IBC). The a-CH<sub>x</sub> and a-CN<sub>x</sub> films were  $\sim 100$  Å thick and were prepared by conventional sputtering using Ar/H<sub>2</sub> or Ar/N<sub>2</sub> gas mixtures of varying composition. The absolute concentrations of hydrogen or nitrogen in the films are not known and they have instead been denoted by the fraction of H<sub>2</sub> (0%, 10%, 15%, 20%) or N<sub>2</sub> (10% or 20%) that was used in the gas mixture for sputtering. Ion beam sputtered films were prepared by using ion beam deposition in which hydrocarbon gas C<sub>x</sub>H<sub>y</sub> is ionized and accelerated toward the substrate. The high deposition energy results in the formation of denser films than those produced by conventional techniques. The cathodic arc films were prepared at the Department of Mechanical Engineering of University of California, Berkeley using a cathodic arc method. The film thickness was  $\sim 75$  Å. Three types of CAC films were used in this work, and the deposition parameters for these films are as shown in Table 1. All films were deposited with a water cooled "minibrute" gun using the following conditions: arc current = 200 A, arc duration = 20 ms, and a substrate bias duty cycle of 2 μs on and 6 μs off. The voltages used during deposition determine the density of

(9) Perry, S. S.; Somarjai, G. A.; Mate C. M.; White, R. *Trib. Lett.* **1995**, *1*, 47.

(10) Paserba, K.; Shukla, N.; Gellman, A. J.; Gui, J.; Marchon, B. *Langmuir* **1999**, *15*, 1709.

(11) Meyers, J. M.; Street, S. C.; Thompson, S.; Gellman, A. J. *Langmuir* **1996**, *12*, 1511.

(12) Shukla, N.; Gellman A. J. In preparation.

**Table 1. Deposition Parameters for the CAC Films**

sample	deposition parameters
CAC 808	100 shots at $-2$ kV
	900 shots at $-100$ V
CAC 810	100 shots at $-2$ kV
	900 shots at $-500$ V
CAC 811	100 shots at $-2$ kV
	900 shots at $-1$ kV

the carbon films with higher voltages corresponding to harder and denser carbon films.

To mount the disk in the UHV chamber a 12.5 mm diameter sample was machine punched from the hard disk and mounted on a sample holder by spot welding with tantalum wires on each side. The sample was heated resistively and cooled to 90 K by mechanical contact with a liquid nitrogen reservoir. The temperature was measured with a chromel–alumel thermocouple spot welded to the back of the sample. The hard disk samples were used as received; however, each sample was heated to 420 K during the bakeout of the UHV chamber, and prior to the TPD experiment the sample was heated to 380 K to remove adsorbed water.

Perfluorodiethylether [(CF<sub>3</sub>CF<sub>2</sub>)<sub>2</sub>O, Aldrich, 99%] is a gas and was used as received. 2,2,2-Trifluoroethanol [CF<sub>3</sub>CH<sub>2</sub>OH, Lancaster Chemicals, 99.5%] was placed in a glass vial and dissolved gases were removed with several freeze–pump–thaw cycles. The purity was then checked by mass spectrometry and the most intense fragment was monitored during the TPD experiment.

Exposure of the sample surface to (CF<sub>3</sub>CF<sub>2</sub>)<sub>2</sub>O or CF<sub>3</sub>CH<sub>2</sub>OH was performed by positioning the sample directly in front of the stainless steel tube attached to the leak valve used to introduce the vapor into the UHV chamber. The distance between the sample and the tube was approximately 3 cm. Reproducible exposures were achieved by keeping the distance between the doser and the sample constant. The accuracy of the exposures was also maintained by using the mass spectrometer to measure the ion signal versus time during the exposure and calculating the area under the signal versus time curve to determine the exposure. All exposures were performed at pressures in the range 10<sup>-9</sup>–10<sup>-8</sup> Torr for periods of 1–200 s and are reported in Langmuirs (1 Langmuir = 10<sup>-6</sup> Torr s).

After adsorption of the species on the sample surface, the TPD spectra were obtained by positioning the sample in front of the mass spectrometer and recording the mass spectrometer signal for a given  $m/q$  ratio during heating of the sample at a constant rate. This serves to measure the rate of desorption versus temperature. The distance between the aperture to the ionizer of the mass spectrometer and the hard disk sample was approximately 2 mm. The mass spectrometer was fitted with a stainless steel cone which had a diameter of 1 cm and therefore detects only the species desorbed from the sample surface.

The a-CN<sub>x</sub> surface was characterized by X-ray photoelectron spectroscopy (XPS). The X-ray source used in these measurements was an 800 W Mg K $\alpha$  ( $h\nu = 1253.6$  eV) source, and a Clam II hemispherical analyzer from VG Scientific was used to measure photoelectron energies. All measurements were made with a pass energy of 50 eV.

### 3. Results

**3.1. TPD of CF<sub>3</sub>CH<sub>2</sub>OH on 20% a-CN<sub>x</sub>.** The desorption of CF<sub>3</sub>CH<sub>2</sub>OH from 20% a-CN<sub>x</sub> films has been studied in order to probe the interactions of Fomblin Zdol end groups with a-CN<sub>x</sub> films. In previous studies, desorption spectra of CF<sub>3</sub>CH<sub>2</sub>OH on a 20% a-CN<sub>x</sub> film were reported at low coverages.<sup>10</sup> Figure 1 shows TPD spectra of CF<sub>3</sub>CH<sub>2</sub>OH on a 20% a-CN<sub>x</sub> obtained using submonolayer to multilayer coverages. In these experiments the 20% a-CN<sub>x</sub> sample was first cooled to a temperature below 90 K and then CF<sub>3</sub>CH<sub>2</sub>OH was adsorbed. The sample was then heated at a constant rate of 2 K/s. Desorption spectra were obtained by using the mass spectrometer to monitor the signal at  $m/q = 31$  (CH<sub>2</sub>OH<sup>+</sup>, CF<sup>+</sup>) as a function of temperature. Other  $m/q$  ratios monitored while the sample

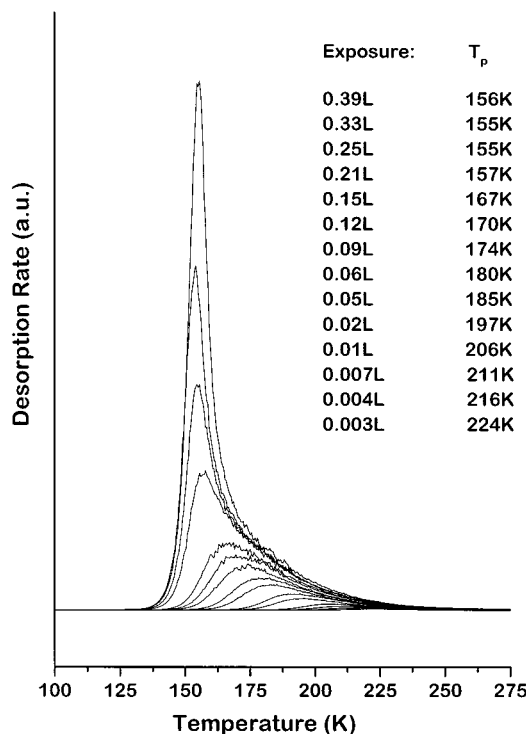


**Figure 1.** TPD spectra of CF<sub>3</sub>CH<sub>2</sub>OH on 20% a-CN<sub>x</sub> obtained with increasing initial coverages. The desorption peak temperature decreases continuously with increasing coverage while the peak amplitude and width increase with coverage. The shift in desorption temperature is a reflection of the heterogeneity of the surface. Adsorption of CF<sub>3</sub>CH<sub>2</sub>OH was performed at 93 K. The heating rate was 2 K/s. The signal monitored was  $m/q = 31$ .

was heated at  $m/q = 69$  (CF<sub>3</sub><sup>+</sup>) and  $m/q = 2$  (H<sub>2</sub><sup>+</sup>). All three fragments exhibited the same desorption profiles for all coverages, suggesting that there is no decomposition of CF<sub>3</sub>CH<sub>2</sub>OH on the a-CN<sub>x</sub> film. At the lowest coverage a single broad peak is observed with a peak temperature at 224 K. At increasing exposures the peaks shifted to lower temperatures and the widths of the peaks increased. The desorption peaks were broad with a width of  $\sim 40$  K. Furthermore, there was also no clear resolution of the monolayer and multilayer desorption features, which makes the determination of the coverages a bit difficult. The desorption of multilayer films is usually characterized by zero-order kinetics with leading or low-temperature edges that are aligned. Since the monolayer and multilayer desorption features are not resolved, we have used the onset of overlapping leading edges to define the onset of multilayer desorption. In the data illustrated in Figure 1 the onset of multilayer desorption occurs at exposures between 0.33 and 0.39 Langmuir. The area under the desorption peak resulting from an exposure of 0.33 Langmuir has been defined as that of the monolayer, and all coverages have been determined by scaling desorption peak areas with respect to that area.

The goal of measuring desorption kinetics as a function of coverage has been to obtain estimates of the differential desorption energy in the coverage range from zero to one monolayer. This can be used as a measure of the heterogeneity in the affinities of the different sites on the a-CN<sub>x</sub> surface for adsorption of CF<sub>3</sub>CH<sub>2</sub>OH. One approach to analyzing the data was to take the difference between a spectrum at one coverage and the spectrum at the next higher coverage. In essence, this gives the desorption spectrum of the increment of CF<sub>3</sub>CH<sub>2</sub>OH added to the surface. The peak desorption temperature obtained by



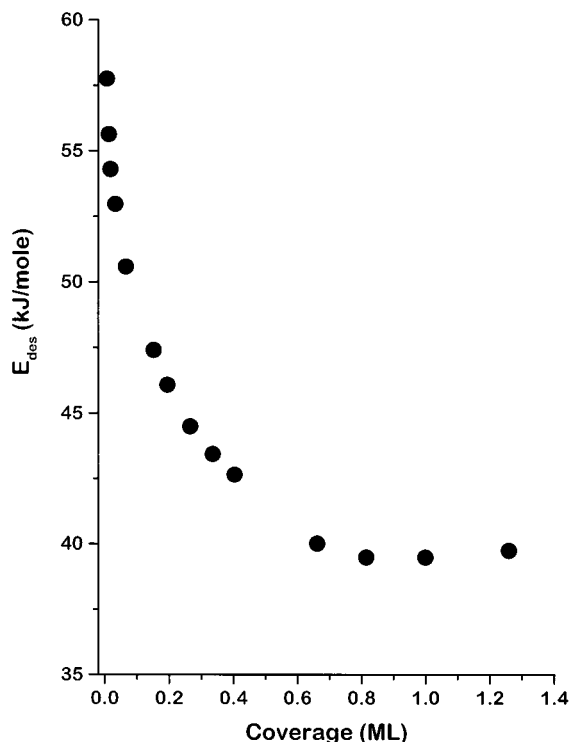


**Figure 2.**  $\text{CF}_3\text{CH}_2\text{OH}$  desorption energies as a function of coverage on the  $\text{a-CN}_x$  film. The desorption energies were obtained from the peak desorption temperature of the TPD spectra in Figure 1. The desorption energy decreases monotonically as the coverage increases.

this method can then be used in conjunction with the Redhead equation to provide a crude estimate of the differential desorption energy at that coverage.<sup>13</sup> The differential desorption spectra are quite noisy; however, we have found that given the shape of the desorption spectra over the range of coverages used, it is possible to simply use the peak desorption temperature for each of the spectra to estimate the desorption temperature of the increment between one coverage and the next. Basically, the  $T_p(\theta)$  curves and hence the  $E_{\text{des}}(\theta)$  obtained by either method are virtually identical. This is probably due to the fact that the peak desorption temperature decreases smoothly and monotonically with coverage while the peak desorption amplitude also increases smoothly and monotonically with coverage. Using the peak desorption temperatures from the data in Figure 1 we have estimated the desorption energy as a function of coverage (Figure 2). This has been done using the Redhead equation assuming that the preexponential for the desorption rate constant is  $10^{13} \text{ s}^{-1}$ . The results plotted in Figure 2 show that the desorption energy decreases smoothly from 56 kJ/mol at the lowest coverage to roughly 39 kJ/mol at the monolayer coverage.

The primary purpose of the plots of desorption energy versus coverage curves generated during the course of this work has been to compare the desorption of  $\text{CF}_3\text{CH}_2\text{OH}$  or  $(\text{CF}_3\text{CF}_2)_2\text{O}$  from the various different carbon films used to protect the surfaces of data storage media. Although there are a number of assumptions and approximations that go into the analysis of the data to determine the  $E_{\text{des}}(\theta)$  curves, these assumptions have been made consistently for all sets of data. Thus we feel that although there may be some systematic error in the absolute values of the desorption energies, these curves

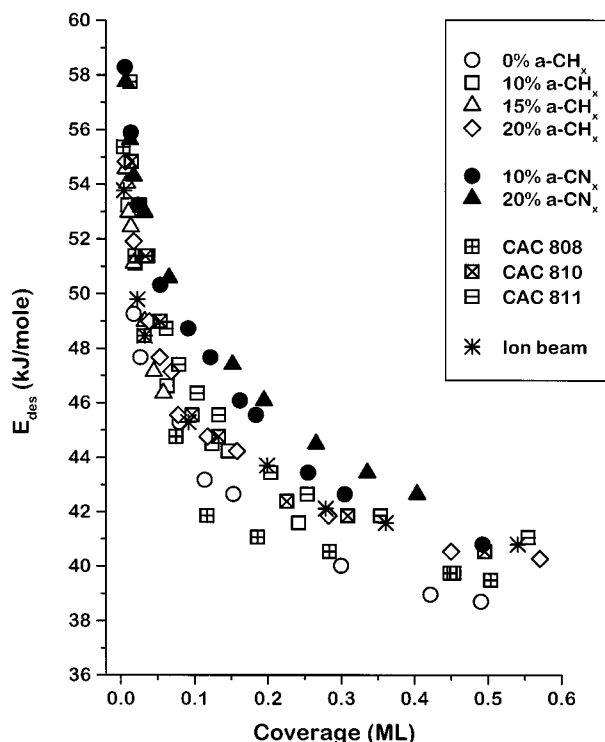


**Figure 3.**  $\text{CF}_3\text{CH}_2\text{OH}$  desorption energies as a function of coverage on  $\text{a-CN}_x$ ,  $\text{a-CH}_x$ , CAC, and IBC films. In all cases the desorption energy decreases monotonically with coverage. The desorption energies on the  $\text{a-CN}_x$  films are slightly higher than those on the other carbon films.

are of use in comparing one adsorbate with another or in comparing desorption from the different surfaces.

**3.2.  $E_{\text{des}}(\theta)$  for  $\text{CF}_3\text{CH}_2\text{OH}$  on all Carbon Films.** The  $E_{\text{des}}(\theta)$  curve for  $\text{CF}_3\text{CH}_2\text{OH}$  on the  $\text{a-CN}_x$  films serves to measure the heterogeneity in the affinities of the different sites on the  $\text{a-CN}_x$  films for adsorption of  $\text{CF}_3\text{CH}_2\text{OH}$ . To determine the desorption energies on the other films and to map out the heterogeneity of the surface adsorption sites, TPD spectra were obtained for  $\text{CF}_3\text{CH}_2\text{OH}$  on all the other films over a range of coverages. Figure 3 shows the  $E_{\text{des}}(\theta)$  curves for  $\text{CF}_3\text{CH}_2\text{OH}$  adsorbed on the various types of carbon films. Note that the percentages listed with the  $\text{a-CN}_x$  and  $\text{a-CH}_x$  films are actually the concentrations of  $\text{N}_2$  and  $\text{H}_2$  in the Ar used to sputter the carbon films onto the disk surface. They do not represent the composition of the films. As observed on the 20%  $\text{a-CN}_x$  film, the  $E_{\text{des}}(\theta)$  of  $\text{CF}_3\text{CH}_2\text{OH}$  decreases smoothly and monotonically with increasing surface coverage. The range of desorption energies observed are between 39 and 58 kJ/mol. The desorption energies of  $\text{CF}_3\text{CH}_2\text{OH}$  are slightly higher on  $\text{a-CN}_x$  films than on  $\text{a-CH}_x$ , CAC, or IBC films. Aside from that difference, however, film composition has little influence on the bonding strength of the  $\text{CF}_3\text{CH}_2\text{OH}$  to the carbon films.

**3.3. TPD of  $(\text{CF}_3\text{CF}_2)_2\text{O}$  on 20%  $\text{a-CN}_x$ .**  $(\text{CF}_3\text{CF}_2)_2\text{O}$  has been used in this study to model the fluoroether linkages of the main chain of Fomblin Zdol. Figure 4 shows the desorption spectra of  $(\text{CF}_3\text{CF}_2)_2\text{O}$  adsorbed on a 20%  $\text{a-CN}_x$  film. As observed for  $\text{CF}_3\text{CH}_2\text{OH}$ , the fluoroethers also have broad desorption peaks and the peak temperature decreases monotonically with increasing exposures. At the same time the peak amplitude increases with increasing exposure. As in the case of  $\text{CF}_3\text{CH}_2\text{OH}$ , the TPD spectra of  $(\text{CF}_3\text{CF}_2)_2\text{O}$  do not resolve the monolayer and multilayer desorption peaks. The onset of multilayer desorption is taken to occur at an exposure of 0.6 Langmuir

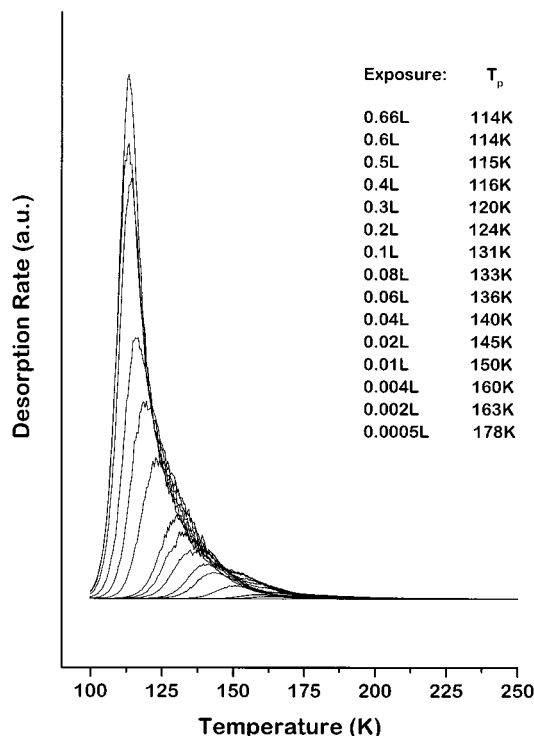


**Figure 4.** TPD spectra of  $(CF_3CF_2)_2O$  on 20% a-CN<sub>x</sub> obtained at increasing initial coverages. The desorption peak temperature decreases with increasing coverage while the peak amplitude and width increase with coverage. Adsorption of  $(CF_3CF_2)_2O$  was performed at 93 K. The heating rate was 2 K/s. The signal monitored was at  $m/q = 69$ .

and is revealed by the overlapping of the low-temperature edges of the desorption curves, indicating the onset of zero-order desorption kinetics. The coverages of  $(CF_3CF_2)_2O$  for the other exposures have been determined by scaling their desorption peak areas to the area of the desorption peak produced by an exposure of 0.6 Langmuir.

**3.4.  $E_{des}(\theta)$  for  $(CF_3CF_2)_2O$  on all Carbon Films.** The objective of measuring the TPD curves for  $(CF_3CF_2)_2O$  over a range of coverages on all the carbon films has been to estimate the desorption energies and the heterogeneity of the adsorption site affinities on the various types of carbon films. Figure 5 shows the  $E_{des}$  as a function of  $(CF_3CF_2)_2O$  coverage on different kinds of carbon overcoats. The range of  $E_{des}$  observed was between 30 and 46 kJ/mol. On each carbon film there is a decrease in the  $E_{des}$  with increasing coverage. The  $E_{des}$  of  $(CF_3CF_2)_2O$  lies in the same range for all the carbon films and it appears that the different carbon compositions do not have a significant effect on the  $E_{des}$  of  $(CF_3CF_2)_2O$ .

**3.5. Disk Surface Composition.** The measurements of the  $(CF_3CF_2)_2O$  and  $CF_3CH_2OH$  desorption energies on the carbon films indicate that there is some degree of heterogeneity to the carbon surfaces and that they expose adsorption sites with different affinities for the adsorbates. This is not surprising given that these are not single crystalline surfaces and that they are not well-defined in composition or structure. It is certainly the case that they contain carbon atoms with both  $sp^2$  and  $sp^3$  hybridization and, in addition, the fact that they have been exposed to air has caused partial oxidation of their surfaces. This is revealed by Figure 6, which shows the X-ray photoelectron spectra of 10% and 20% a-CN<sub>x</sub> films. The C(1s), N(1s), and O(1s) regions of the spectra were recorded and the area under the XP peak was integrated after a Shirley subtraction of the background. The integrated areas are shown in the Table 2 with the relative concentrations of

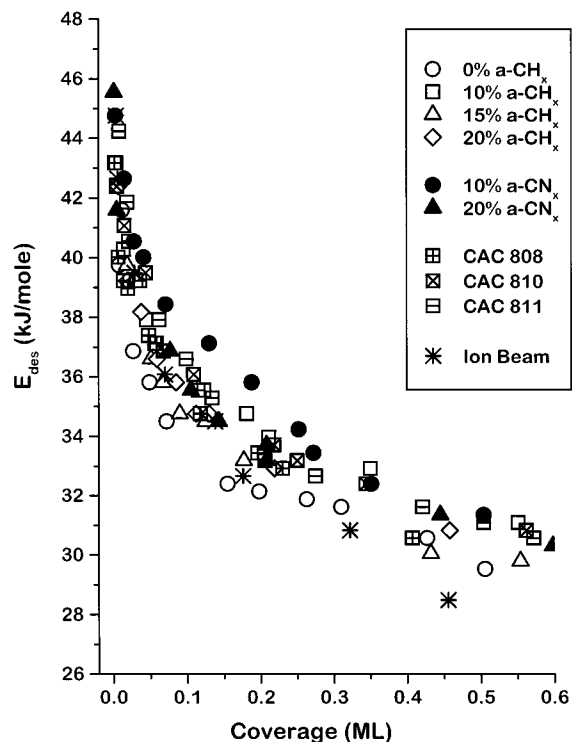


**Figure 5.** Desorption energy as a function of coverage for  $(CF_3CF_2)_2O$  adsorbed on a-CN<sub>x</sub>, a-CH<sub>x</sub>, CAC, and IBC films. The desorption energies all decrease monotonically with coverage and seem to indicate the same distribution of binding site affinities on all the carbon films.

nitrogen and oxygen at the surfaces of the films. These numbers indicate that the nitrogen concentrations at the surfaces of the films were about 15–20% and the oxygen concentrations at the surfaces of the films were about 10–15%.

## 4. Discussion

**4.1. Surface Heterogeneity.** The desorption peaks observed for both  $(CF_3CF_2)_2O$  and  $CF_3CH_2OH$  adsorbed on all carbon films are broad. In comparison, the desorption peaks observed for  $(CF_3CF_2)_2O$  and  $CF_3CH_2OH$  on Cu(111) or graphite surfaces are very narrow with well-resolved monolayer and multilayer features.<sup>11,12,14</sup> The breadth of the desorption features prohibits distinguishing between monolayer and multilayer desorption features in the manner done on single-crystal surfaces. In principle, the breadth of the desorption features could be due to heterogeneity of the carbon films or due to repulsive interactions between molecules adsorbed on these surfaces. One of main points of this work is to make the case that the breadth of these desorption features is due to heterogeneity rather than repulsive interactions between adsorbates. Comparisons of the TPD on the amorphous carbon surfaces with those obtained from single crystalline Cu(111) and graphite surfaces make it quite apparent that this is the case. On those homogeneous surfaces the desorption peaks are quite narrow and if anything indicate that the interactions between the adsorbed  $(CF_3CF_2)_2O$  molecules or adsorbed  $CF_3CH_2OH$  molecules are attractive.<sup>11,12</sup> The  $E_{des}(\theta)$  curves of Figures 3 and 5 reveal that the magnitude of this heterogeneity in adsorption affinity is roughly similar on all the amorphous carbon films.

The heterogeneity in the types of adsorption sites and their affinities for  $(CF_3CF_2)_2O$  and  $CF_3CH_2OH$  adsorption

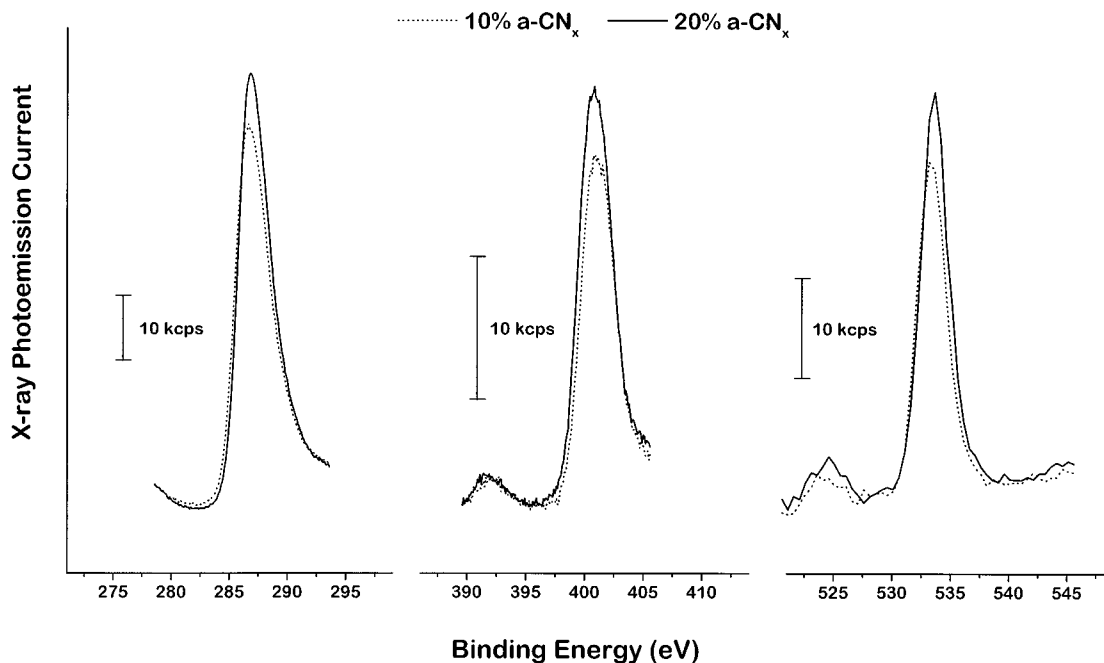


**Figure 6.** X-ray photoelectron spectra of C(1s), N(1s), and O(1s) peaks from 10% and 20% a-CN<sub>x</sub> films. These indicate the presence of roughly equivalent nitrogen concentrations in the films and relatively high concentrations of oxygen.

**Table 2. X-ray Photoelectron Spectra of C(1s), N(1s), and O(1s) on 10% and 20% a-CN<sub>x</sub> Films**

sample	C(1s) signal	N(1s) signal	% N in film	O(1s) signal	% O in film
10% a-CN <sub>x</sub>	224 000	75 900	15%	120 000	15%
20% a-CN <sub>x</sub>	206 000	89 200	18%	103 000	14%

can be due in part to different hybridization of carbon atoms. The carbon films generally include a mixture of sp<sup>3</sup>, sp<sup>2</sup> and sp hybridized carbon atoms.<sup>14</sup> In addition there can be different functional groups present at the surface due to oxidation. Yanagisawa has proposed that there are a variety of oxygen-containing functional groups such as CO, OH, or CO<sub>2</sub>H and unpaired electrons or dangling bonds on carbon surfaces.<sup>15</sup> The dangling bonds were found to be effective adsorption sites for PFPE lubricants. He also reported a correlation between the heat of adsorption of PFPE diol and the dangling bond density of carbon. The heat of adsorption was observed to be lowest in graphite with sp<sup>2</sup> hybridized carbon. It was highest on diamond with a purely sp<sup>3</sup> structure but having dangling bonds at grain boundaries or dislocations. Several other reports of the presence of dangling bonds in carbon films have been published.<sup>16–18</sup>

Unlike amorphous carbon films, graphite has only sp<sup>2</sup> hybridized carbon and is homogeneous. As expected for a homogeneous surface, the desorption of both (CF<sub>3</sub>CF<sub>2</sub>)<sub>2</sub>O and CF<sub>3</sub>CH<sub>2</sub>OH from the graphite surface exhibits well-defined and sharp monolayer and multilayer peaks. The desorption peaks from graphite<sup>12</sup> are narrow and are similar to those observed on any single-crystal metal surface. The desorption peak width was observed to be ~10 K, which is about 30 K less than that observed on the amorphous carbon films studied in this work. In addition, the peak desorption temperatures from the graphite

surface were observed to increase with increasing coverage of both (CF<sub>3</sub>CF<sub>2</sub>)<sub>2</sub>O and CF<sub>3</sub>CH<sub>2</sub>OH, suggesting that there are attractive rather than repulsive interactions between the molecules. This further justifies our explanation of the breadth of the desorption peaks as arising from a variety of adsorption sites on the amorphous carbon films rather than repulsive interactions between molecules.

**4.2. Effects of Film Composition on Ether and Alcohol Adsorption.** Our study has shown that varying either the hydrogen or nitrogen content in the amorphous carbon films does not have a strong influence on the adsorption of either (CF<sub>3</sub>CF<sub>2</sub>)<sub>2</sub>O or CF<sub>3</sub>CH<sub>2</sub>OH. Our previous attempt to vary the hydrogen concentration in the carbon films used annealing in a vacuum to reduce the hydrogen concentration.<sup>8</sup> In that experiment it was observed that increasing the annealing temperature from 550 to 700 K, while certainly reducing the hydrogen concentration of the film, also caused an increase in the desorption energy of the fluoroethers from the surfaces of these films. The results presented in this work indicate that that increase in the desorption energy cannot be attributed to the decrease in hydrogen concentration and must have been due to some other changes in the carbon films that occurred during annealing. Heating of a-CH<sub>x</sub> films to temperatures of up to 750 K not only removes hydrogen but also removes other contaminants such as water vapor and oxygen from the surface and also tends to induce graphitization of the carbon film. These changes must be responsible for the previously reported changes in the desorption energies of the ethers that resulted from heating.

**4.3. Differences between Alcohol and Ether Adsorption.** On all the carbon films studied in this work we have observed that the desorption energy of CF<sub>3</sub>CH<sub>2</sub>OH is greater than that of (CF<sub>3</sub>CF<sub>2</sub>)<sub>2</sub>O. Previous work has shown that these two molecules interact with the surface by different mechanisms. The ethers adsorb by electron pair donation from the ether oxygen linkage while the alcohols adsorb by hydrogen bonding of the hydroxyl group to the surface.<sup>8,10</sup> The results of this work suggest that the strength of the interaction of the hydroxyl groups that

(15) Yanagisawa, M. *Trib. Mech. Magn. Storage System, STLE Publ.* **1994**, *9*, 36.

(16) Wada, N.; Gaczi, P. J.; Solin, S. A. *J. Non-Cryst. Solids* **1980**, *35*, 543.

(17) Miller, D. J.; Mackenzie, D. R. *Thin Solid Films* **1983**, *108*, 257.

(18) Jansen, F.; Machonkin, M.; Kaplan, S.; Hark S. *J. Vac. Sci. Technol.* **1985**, *A3*, 6.

terminate the Fomblin Zdol chain are greater than the individual interactions of the ether linkages that make up the main chain of Fomblin Zdol. This is consistent with studies of surface diffusion. O'Connor and others<sup>19–21</sup> investigated surface diffusion of PFPE on silicon and carbon films as a function of film thickness, chain functionality, temperature, humidity, and molecular weight. They reported that the activation energy for surface diffusion ( $E_{diff}$ ) of Fomblin Zdol (50.6 kJ/mol) was higher than that of Fomblin Z15 (20.6 kJ/mol), indicating a stronger affinity of the hydroxyl end group for the silicon wafers. The Fomblin Z15 is terminated with  $CF_3$  groups rather than hydroxyl groups. If the interaction of the end groups with the carbon film is stronger than the interaction of the main chain, then this suggests that at high coverages Fomblin Zdol can adopt a structure in which it is just the end groups that are interacting with the carbon film while the main chains interact with one another. This is depicted in Figure 7. This structure is consistent with that proposed on the basis of diffusion measurements in which thick films of Fomblin Zdol tended to form layered structures on the carbon film surface. The first layer was believed to interact with the carbon film through hydrogen bonding of the hydroxyl group, in much the same manner as we have depicted.<sup>22</sup>

### 5. Conclusions

The surfaces of the amorphous carbon films used to protect magnetic data storage media have been shown to

(19) O'Connor, T. M.; Young, R. B.; Jhon, M. S.; Min, B. G.; Yoon, D. Y.; Karis, T. E. *J. Appl. Phys.* **1999**, *79*(8), 5788.

(20) Ma, X.; Gui, J.; Smoliar, L.; Grannen, K.; Marchon, B.; Bauer, C. L.; Jhon, M. S. *Phys. Rev. E* **1996**, *59*, 722.

(21) Ma, X.; Gui, J.; Grannen, K.; Smoliar, L.; Marchon, B.; Jhon, M. S.; Bauer, C. L. *Trib. Lett.* **1999**, *6*, 9.

(22) Ma, X.; Gui, J.; Smoliar, L.; Grannen, K.; Marchon, B.; Jhon, M. S.; Bauer, C. L. *J. Chem. Phys.* **1999**, *110*, 3129.

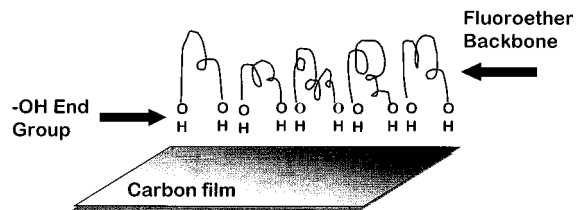


**Figure 7.** Structural schematic of Fomblin Zdol adsorbed on a carbon film. Since the hydroxyl end groups have stronger interactions with the carbon films than the ether linkages of the main chain, at high coverages the Fomblin Zdol will tend to adopt a geometry which favors end group interaction with the surface. This means that the molecules could adopt a structure in which the main chains are not interacting directly with the surface.

be heterogeneous in the sense that they expose adsorption sites with a range of affinities for interaction with the ether linkages and hydroxyl end groups of Fomblin Zdol. The interaction of the hydroxyl end groups of Zomblin Zdol with amorphous carbon films is stronger than the interaction of the ether linkages of the backbone. The distribution of binding site affinities is quite similar among the various types of  $a-CH_x$ ,  $a-CN_x$ , CAC, and IBC films. The exception is that the interaction of the hydroxyl end groups is slightly stronger with the  $a-CN_x$  films than with the  $a-CH_x$  films.

**Acknowledgment.** We would like to acknowledge the support of Seagate Technology, Inc., and their donation of the  $a-CH_x$  films and also the Data Storage System Center of Carnegie Mellon University, for support of this work through grant no. ECD-8907068 from the National Science Foundation. We would like to thank Walton Fong and David Bogy for preparation and supply of the CAC films.

LA0004496